

## Blooms of *Prorocentrum donghaiense* reduced the species diversity of dinoflagellate community

Huan Wang<sup>1,3</sup>, Zhangxi Hu<sup>1,2,4</sup>, Zhaoyang Chai<sup>1,2,4</sup>, Yunyan Deng<sup>1,2,4</sup>, Zifeng Zhan<sup>5</sup>, Ying Zhong Tang<sup>1,2,4\*</sup>

<sup>1</sup> CAS Key Laboratory of Marine Ecology and Environmental Sciences, Institute of Oceanology, Chinese Academy of Sciences, Qingdao 266071, China

<sup>2</sup> Laboratory for Marine Ecology and Environmental Science, Pilot National Laboratory for Marine Science and Technology (Qingdao), Qingdao 266237, China

<sup>3</sup> University of Chinese Academy of Sciences, Beijing 100049, China

<sup>4</sup> Center for Ocean Mega-Science, Chinese Academy of Sciences, Qingdao 266071, China

<sup>5</sup> Department of Marine Organism Taxonomy and Phylogeny, Institute of Oceanology, Chinese Academy of Sciences, Qingdao 266071, China

Received 24 November 2018; accepted 19 February 2019

© Chinese Society for Oceanography and Springer-Verlag GmbH Germany, part of Springer Nature 2020

### Abstract

Most of reported harmful algal blooms (HABs) of microalgae (75%) have been caused by dinoflagellates. Studies on the negative effects of HABs have generally focused on animals, valuable organisms in particular, and environmental factors such as dissolved oxygen and nutrients, but relatively fewer on community level, particularly that using metagenomic approach. In this study, we reported an investigation on the effects of a HAB caused by the dinoflagellate *Prorocentrum donghaiense* on the species diversity and community structure of the dinoflagellate sub-community via a pyrosequencing approach for the samples taken before, during, and after the bloom season of *P. donghaiense* in the East China Sea. We sequenced partial 28S rRNA gene of dinoflagellates for the field samples and evaluated the species richness and diversity indices of the dinoflagellate community, as a sub-community of the total phytoplankton. We obtained 800 185 valid sequences (categorized into 560 operational taxonomic units, OTUs) of dinoflagellates from 50 samples and found that the biodiversity of dinoflagellate community was significantly reduced during the blooming period in comparison to that in pre- and after-blooming periods, as reflected in the four diversity indices: the species richness expressed as the number of OTUs, Chao1 index, Shannon index (evenness), and Gini-Simpson index. These four indices were all found to be negatively correlated to the cell density of the bloom species *P. donghaiense*. Correlation analyses also revealed that the *P. donghaiense* cell abundance was correlated negatively with  $\text{NO}_3^-$ -N, and  $\text{NO}_2^-$ -N, but positively with total nitrogen (TN) and total phosphorus (TP). Principal coordinates analysis (PCoA) showed that the community structure of dinoflagellates was markedly different among the different sampling periods, while the redundancy analysis (RDA) revealed *P. donghaiense* abundance, salinity,  $\text{NO}_3^-$ -N, and  $\text{SiO}_3^{2-}$  were the most four significant factors shaping the dinoflagellate community structure. Our results together demonstrated that HABs caused by the dinoflagellate *P. donghaiense* could strongly impact the aquatic ecosystem on the sub-community level which the blooming species belongs to.

**Key words:** *Prorocentrum donghaiense*, dinoflagellate community, diversity, pyrosequencing, East China Sea

**Citation:** Wang Huan, Hu Zhangxi, Chai Zhaoyang, Deng Yunyan, Zhan Zifeng, Tang Ying Zhong. 2020. Blooms of *Prorocentrum donghaiense* reduced the species diversity of dinoflagellate community. Acta Oceanologica Sinica, 39(4): 110–119, doi: 10.1007/s13131-020-1585-1

### 1 Introduction

Harmful algal blooms (HABs) have been increasing globally in extension and impacts on public health, aquaculture industry, fisheries, and ecosystems such as oxygen depletion, reduction in water quality (Anderson et al., 2012, 2002; Smayda, 1990). Among all HABs-causing species, dinoflagellates are the most important

contributors, as about 75% of reported HABs were caused by dinoflagellates (Smayda, 1997). Dinoflagellates have a number of characteristic features (Burkholder et al., 2006) and are one of the most important primary producers and a vital component of coral reef symbiotic system (Aranda et al., 2016; Lin et al., 2015). While HAB events may be caused by a variety of environmental

Foundation item: The National Natural Science Foundation of China under contract Nos 61533011 and 41776125; the NSFC-Shandong Joint Fund for Marine Ecology and Environmental Sciences under contract No. U1606404; the Scientific and Technological Innovation Project of the Qingdao National Laboratory for Marine Science and Technology under contract No. 2016ASKJ02; the National Key R&D Program of China under contract No. 2017YFC1404300; the Creative Team Project of the Laboratory for Marine Ecology and Environmental Science, Qingdao National Laboratory for Marine Science and Technology under contract No. LMEES-CTSP-2018-1.

\*Corresponding author, E-mail: [yingzhong.tang@qdio.ac.cn](mailto:yingzhong.tang@qdio.ac.cn)

and autecological factors such as illumination, water temperature, nutrients availability, growth rate, vertical migration, and special life history (Anderson et al., 2002; Xu et al., 2010), as feedbacks, HABs may cause many negative effects on the ecosystems that can be viewed from different levels (from ecosystem, community to sub-cellular and molecular levels) and aspects (physical, chemical, biological, public health, and economic). In general, previous studies on the negative effects of HABs have been mainly focused on fisheries, aquaculture, and human public health (Anderson et al., 2012; Landsberg, 2002), relatively fewer studies, however, have investigated the effects of HABs on the

level of community, and even fewer using high throughput meta-genomic approach, such as phytoplankton community diversity, community structure, function and stability (Cui et al., 2018; Zhou et al., 2018). This oddness was at least partly due to the limitations in how to obtain comprehensive lists of species and identify species of small sizes, simple or similar morphologies, low abundances, and to process numerous samples efficiently. Conventional methods for identifying and quantifying phytoplankton species from field samples generally involved in the use of light microscopy, and sometimes were aided with flow cytometry and alike, pigment analysis, however they all have limita-

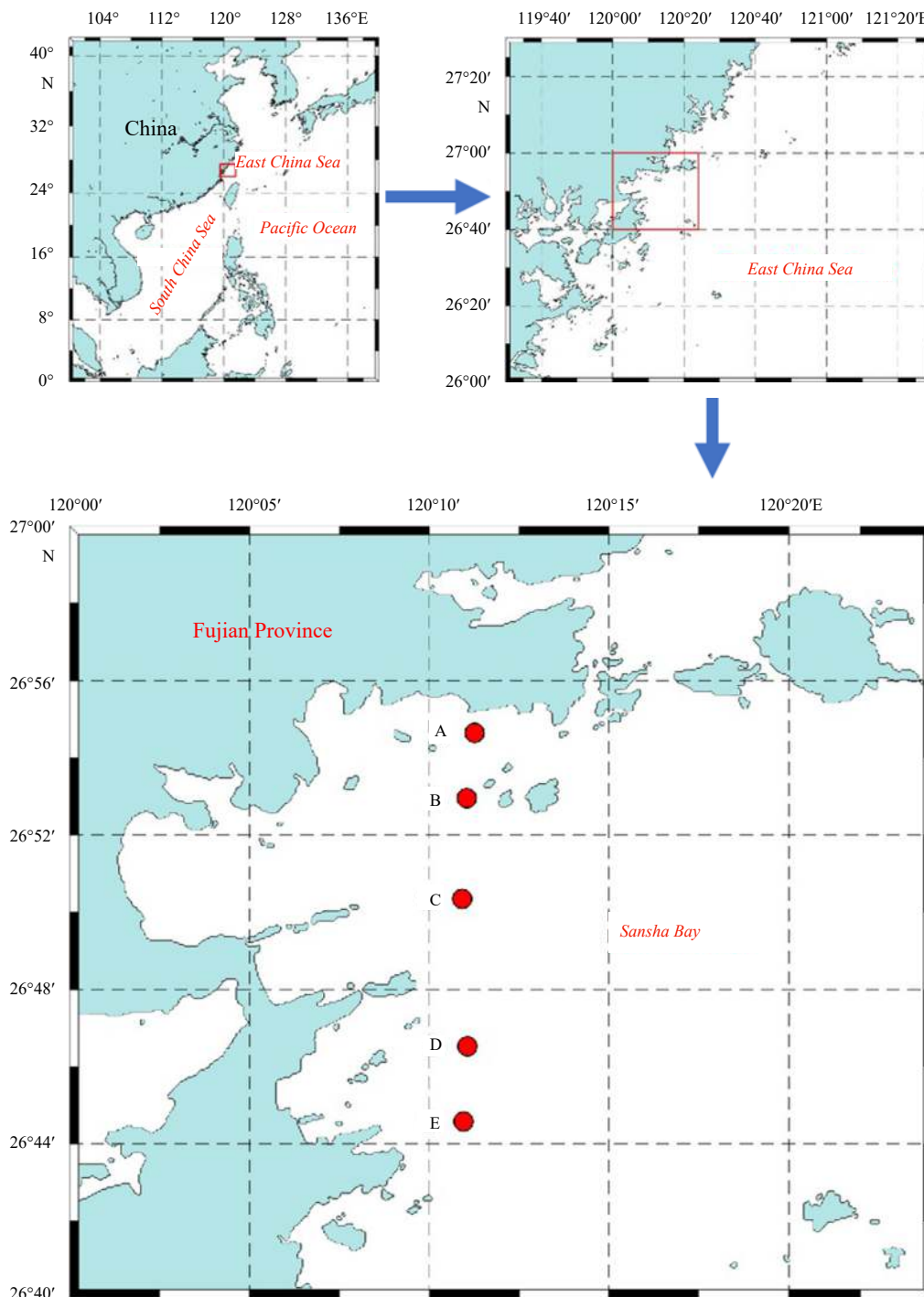


Fig. 1. Locations of sampling sites in the Sansha Bay, Ningde, China.

**Table 1.** Categorization of samples according to sampling timing (pre-, during, and after blooms) and locations

	0331 Non-blooming	0422 Blooming	0503 Blooming	0513 Blooming	0531 Non-bloomig	0719 Non-blooming
Sample ID	A0331a	A0422a	E0503a	A0513a	A0531a	A0719a
	A0331b	A0422b	E0503b	A0513b	A0531b	A0719b
	B0331a	B0422a	A0503a	B0513a	B0531a	B0719A
	B0331b	B0422b	A0503b	B0513b	B0531b	B0719b
	C0331a	C0422a	B0503a	C0513a	C0531a	C0719a
	C0331b	C0422b	B0503b	C0513b	C0531b	C0719b
	D0331a	D0422a	C0503a	D0513a	D0531a	D0719a
	D0331b	D0422b	C0503b	D0513b	D0531b	D0719b
			D0503a			
			D0503b			

tions in identifying and quantifying those species of highly small sizes, simple or similar morphologies, low abundances, and novel taxa that have not been described (Chai et al., 2018). With the development of molecular approaches, high-throughput gene sequencing (e.g., 18S and 28S rRNA genes) have recently been increasingly applied to environmental samples to conquer these limitations (Chai et al., 2018, 2020; Vaultot et al., 2008; Xu et al., 2017; Zhou et al., 2018). The well-developed, high-throughput sequencing allows us to deeply sequence environmental samples and to sensitively and accurately identify species, and thus detect slight changes at the community level (Miao et al., 2017; Schneider et al., 2017; Sunagawa et al., 2015).

In this study, we investigated the effects of blooms of a common HABs-causing dinoflagellate in China, *Prorocentrum donghaiense*, on the dinoflagellate sub-community level, which the bloom species belongs to, in terms of species richness and other biodiversity indices by applying a high-throughput amplicon sequencing approach. We applied a pair of particularly designed primers targeting the large subunit rRNA gene to sequencing the samples taken before, during, and after *P. donghaiense* blooming from the Sansha Bay, Fujian Province, China. We also measured other variables including cell density of *P. donghaiense*, chlorophyll content, nutrients (total nitrogen (TN), nitrate ( $\text{NO}_3^-$ -N), nitrite ( $\text{NO}_2^-$ -N), ammonium ( $\text{NH}_4^+$ -N), total phosphorus (TP), phosphate ( $\text{PO}_4^{3-}$ -P), silicate ( $\text{SiO}_3^{2-}$ )), salinity, and temperature to examine the interactions among these variables, *P. donghaiense* blooms, and the dinoflagellates community succession.

## 2 Materials and methods

### 2.1 Sampling sites, dates and procedures

The study area, Sansha Bay, is located at the northeast to Ningde, Fujian Province ( $26^\circ44.5' - 26^\circ54.5' \text{N}$ ,  $120^\circ10.9' - 120^\circ11.3' \text{E}$ ), one of Fujian Province's major aquaculture water in the East China Sea (Fig. 1), where has observed highly frequent HABs caused by *P. donghaiense*, *Karenia mikimotoi*, and, occasionally, other species (Lin et al., 2014; Lu et al., 2005; Yao et al., 2006). There were about 161 HAB incidents during 2001–2010 and 65 events between 2011 and 2015, amongst them *P. donghaiense* being the main causative species (State Oceanic Administration, 2001–2015).

From March to July, 2016, we conducted six cruises and collected a total of 50 samples, which covered pre-, during, and post-bloom periods. Four or five sampling sites were selected in the study area (Table 1). March 31 (0331) was a time prior to the bloom, the dates April 22 (0422), May 3 (0503), May 13 (0513) were categorized as during-bloom period based on cell counts of *P. donghaiense*, with May 3 observing the peak of a bloom, and May 31 (0531) and July 19 (0719) were categorized as post-bloom

period. Here, we simply define a bloom according to chlorophyll *a* (Chl *a*) content and dominant specie concentration, with Chl *a* content higher than  $5 \mu\text{g/L}$  when there is a dominant species (Jonsson et al., 2009) and 20 000 cells/mL of the dominant species, with an awareness of no commonly accepted standard of cell density to define a bloom. The sample IDs include sampling sites (A, B, C, D, E), sampling dates (0331, 0422, 0503, 0513, 0531, 0719), and the duplicate letters a and b. For example, the sample ID A0331a refers to the first sample taken on March 31 from Site A.

Water temperature and salinity were measured on site using a hand-held thermometer (BoBang Ltd, China) and a refractometer (Atago Ltd, Japan). Water samples were taken from 0.5 m below the surface and transferred into 5 L polyethylene bucket. Plankton samples for DNA extraction were collected by filtering 1.5 L water through a hydrophilic polycarbonate membrane (47 mm diameter,  $0.4 \mu\text{m}$  pore size, Merck Millipore Ltd, Germany) with duplicates, put into an icebox and then  $-20^\circ\text{C}$  immediately after arriving the laboratory and then stored at  $-80^\circ\text{C}$  until DNA extraction. Water samples (1 L) were also fixed with Lugol's iodine solution (final concentration, 2%) for counting cells of *P. donghaiense* using plankton counting chamber under an inverted light microscope (IX73, Olympus, Tokyo, Japan). Samples for  $\text{NO}_3^-$ -N,  $\text{NO}_2^-$ -N,  $\text{NH}_4^+$ -N,  $\text{PO}_4^{3-}$ -P, and  $\text{SiO}_3^{2-}$  were filtered through Whatman GF/C filters (pore size  $\sim 1.2 \mu\text{m}$ ), and added 2 drops of chloroform per 100 mL sample. Samples for TN (total nitrogen) and TP (total phosphorous) were pretreated by adding two drops of 98% sulfuric acid per 100 mL sample. Samples for Chl *a* (at least 500 mL for each sample) were filtered onto Whatman GF/F glass fiber filters (pore size  $\sim 0.7 \mu\text{m}$ ) and frozen until analysis. All samples were immediately transported to the laboratory in cold conditions and subjected to measurements of the nutrients and Chl *a*.

### 2.2 Measurements of nutrients and other variables

$\text{NO}_3^-$ -N,  $\text{NO}_2^-$ -N,  $\text{NH}_4^+$ -N,  $\text{PO}_4^{3-}$ -P, and  $\text{SiO}_3^{2-}$  were analyzed colorimetrically using a nutrient analyzer (Skalar Ltd, Netherland) according to the protocols of JOGFS report No. 19 (JOGFS International Project Office, 1994). For TN and TP analyses, samples were digested using potassium persulfate under high temperature ( $115^\circ\text{C}$ , 30 min) according to the standard protocol (Valderrama, 1981), and then the treated samples were also analyzed colorimetrically using the nutrient analyzer. Chl *a* was extracted with 90% aqueous acetone, and measured fluorometrically using a Turner Designs fluorometer (Parsons et al., 1984).

### 2.3 Primer design, DNA extraction, PCR amplification, and pyrosequencing

The forward and reverse primers were designed to target the partial 28S rRNA gene (rDNA) including the highly variable D2

domain mainly for dinoflagellates. Reference sequences of 28S rDNA for microalgae of different groups and ciliates were selected and aligned with that of dinoflagellates to verify the suitability of the selected oligonucleotide sequences as primers using Primer 3 (Rozen and Skaletsky, 2000). The specificity of the generated primer candidates were checked against the GenBank sequence collection by a standard nucleotide-nucleotide BLAST search for the sake of amplifying all dinoflagellates, resulting in the primers as follows: forward primer LSU347 (5'-CAAGTAC-CATGAGGGAAA-3') and reverse primer LSU929 (5'-ACGAACGATTGACGTCAGTA-3').

Genomic DNA was extracted with a plant DNA extraction kit (Tiangen, Beijing, China) according to the manufacturer's protocol. PCR was then conducted in 20  $\mu$ L reaction mixture containing 2  $\mu$ L of deoxynucleoside triphosphate at a concentration of 2.5 mmol/L, 0.8  $\mu$ L of forward and reverse primers (5  $\mu$ mol/L each), respectively, 0.4  $\mu$ L FastPfu Polymerase, 5 $\times$  FastPfu Buffer 4  $\mu$ L, and 1  $\mu$ L of template DNA (final amount 10 ng) under the following PCR conditions: 94°C for 5 min, 35 cycles of 94°C for 30 s, 46°C for 30 s, and 72°C for 30 s and 72°C for 10 min extension. PCR amplicons were purified with an AxyPrep DNA gel extraction kit (Axygen, USA) and quantified using the QuantiFluor-ST Fluorescence quantitative system (Promega, USA). Amplicons from different water samples were then mixed to achieve equal

mass concentrations in the final mixture, which was then pyrosequenced using a 454 Genome Sequencer (GS) FLX Titanium platform (LC-Bio Technology Co. Ltd, Hangzhou, China) as previously described (Sun et al., 2014). FASTA-formatted sequences and corresponding quality scores (QC) were extracted from the ".sff" data file using the GS Amplicon software package. Raw sequencing data of this study have been deposited in the NCBI database under Accession No. SRR8163577.

#### 2.4 Statistics and bioinformatic analyses

Aligned sequences were clustered into operational taxonomic units (OTUs) defined by 97% similarity (identity) using the average neighbor algorithm. The taxonomy assignment of OTUs was done by Global Alignment for Sequence Taxonomy (GAST) process (Huse et al., 2008). Community diversity parameters ((Shannon index, Gini-Simpson index (1- $\lambda$ ), and Chao1 index (as an asymptotic species richness estimator)) for each sample were calculated as described in the Mothur software manual (<http://www.mothur.org/>). Principal coordinates analysis (PCoA) were conducted at the OTU level with the community ecology package (<http://www.mothur.org/>). Redundancy analysis (RDA) was performed to analyze the major environmental factors affecting the community structure using the R-vegan and R-map tools for Linux (Legendre et al., 2011). Spearman's rank correlation coeffi-

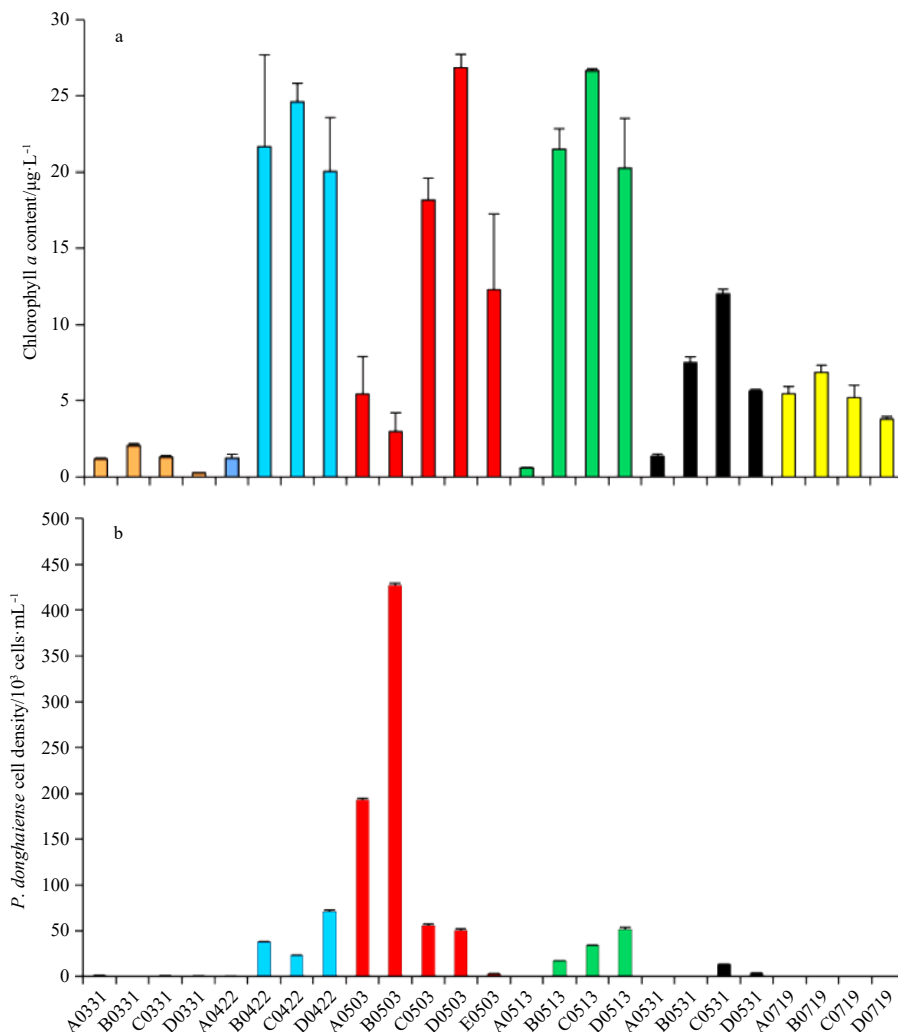


Fig. 2. The cell density of *P. donghaiense* and the chlorophyll *a* of different samples in the coastal waters of the Sansha Bay, Ningde, China. Error bars indicate  $\pm 1 \times \text{SD}$ . a. Chlorophyll *a*, and b. cell density of *P. donghaiense*.

**Table 2.** The ratio of dissolved inorganic nitrogen (DIN) to dissolved inorganic phosphorus (as  $\text{PO}_4^{3-}\text{-P}$ ) (DIN/DIP)

Date	Max	Min	Mean $\pm$ SD
0331	21.5	18.8	20.4 $\pm$ 1.2
0422	17.8	4.0	8.3 $\pm$ 6.4
0503	14.6	3.4	6.9 $\pm$ 5.2
0513	5.8	3.4	4.1 $\pm$ 1.2
0531	46.9	7.4	27.4 $\pm$ 19.7
0719	9.9	4.7	7.0 $\pm$ 2.2

cient (or Spearman's rho) was calculated to measure possible correlation between two variables using the software SPSS 22.0. Since the Spearman correlation evaluates the monotonic relationship between two variables that they may tend to change together but not necessarily at a constant rate, we chose to use the Spearman correlation coefficient, as we assumed that the two variables might be correlated but not necessarily correlated linearly. The significance level was set at 0.05 for all tests unless otherwise stated.

### 3 Results

#### 3.1 Variations and dynamics of *P. donghaiense* cell density, Chl *a* content, and nutrients

During the six cruises from March to July of 2016, *P. donghaiense* reached the maximum cell density of  $\sim 4.3 \times 10^5$  cells/mL on May 3 (Fig. 2). The cell density of *P. donghaiense* was 270 cells/mL on March 31 (pre-blooming) and the lowest cell density of 83 cells/mL was on July 19 (after blooming). During the blooming period of late April to early May, *P. donghaiense* abundance ranged from 300 to  $\sim 4.3 \times 10^5$  cells/mL. However, among the sampling sites, *P. donghaiense* cell density varied significantly, with Site B or Site C having significantly higher abundance than that of Site A ( $p < 0.05$ ).

The Chl *a* level ranged from 0.3 to 26.8  $\mu\text{g/L}$ , with the highest observed at Site D on May 3, where and when the bloom of *P. donghaiense* was observed (with a cell density of *P. donghaiense*  $\sim 5.0 \times 10^4$  cells/mL). There existed a significant positive correlation between *P. donghaiense* cell density and Chl *a* (Spearman rho=0.54,  $p < 0.05$ ), indicating *P. donghaiense* was one of, but not the only, major contributors of phytoplankton biomass. Strikingly, it is noteworthy that for the sample B0503, there was a discrepancy between Chl *a* and the cell abundance of *P. donghaiense* (Fig. 2), which we think was possibly due to a lower Chl *a* content per cell for *P. donghaiense* relative to that of other phyto-

plankton species such as diatoms and green microalgae because of the highly small-sized cells and pigment composition of *P. donghaiense*. In addition, the extremely high abundance of *P. donghaiense* during the blooming period (e.g., early May) also decreased the abundance of other phytoplankton with higher Chl *a* content per cell.

Water temperature ranged from 13.9°C to 29.5°C during the sampling period. No significant correlation was observed between water temperature and Chl *a* (Spearman rho=0.16,  $p > 0.05$ ), neither between temperature and *P. donghaiense* cell density (Spearman rho=-0.19,  $p > 0.05$ ). Regarding the correlations between nutrients and *P. donghaiense* cell density, we observed no correlation for  $\text{NH}_4^+\text{-N}$  and  $\text{PO}_4^{3-}\text{-P}$ , but *P. donghaiense* cell density significantly correlated with  $\text{NO}_3^-\text{-N}$ ,  $\text{NO}_2^-\text{-N}$ , TN, TP, and  $\text{SiO}_3^{2-}$ , respectively ( $p < 0.05$ ), with  $\text{NO}_3^-\text{-N}$  and  $\text{NO}_2^-\text{-N}$  being negative (Spearman rho=-0.59 and -0.60, respectively;  $p < 0.05$ ), and TN, TP, and  $\text{SiO}_3^{2-}$  being positive (Spearman rho=0.75, 0.84, and 0.51, respectively;  $p < 0.05$ ), indicating N and P as supporting or driving factors for the bloom of *P. donghaiense*. The ratios of dissolved inorganic nitrogen (DIN, the sum of  $\text{NO}_3^-\text{-N}$ ,  $\text{NO}_2^-\text{-N}$  and  $\text{NH}_4^+\text{-N}$ ) to dissolved inorganic phosphorus (DIP, as  $\text{PO}_4^{3-}\text{-P}$ ) in the surface water tended to decrease along with the development and maintenance of bloom (Table 2). At the beginning of the survey (March 31), the DIN to DIP ratios in the surface layer was 18–22 on average, while, during the blooming period of *P. donghaiense*, the ratio showed a downward trend in general. On May 13, the ratio reached the minimum (3.4, Table 2). There existed a significant negative correlation between *P. donghaiense* cell density and DIN/DIP (Spearman rho=-0.64;  $p < 0.05$ ).

#### 3.2 General description for pyrosequencing results

A total of 800 185 valid sequence reads of dinoflagellates with an average length of about 400 bp were generated from the 50 samples (Table S2). By clustering the unique sequences at 97% similarity level, these dinoflagellate sequences were grouped into 560 OTUs, with the number of OTUs ranging from 39 to 304 per sample. The highest richness was observed in the sample C0719b (after bloom) and the lowest richness was observed in A0503b (during bloom). OTU richness decreased during the blooming period from April 22 to May 13, and then increased with the disappearance of bloom from May 31 to July 17, and the Chao1 index (an indicator of total species richness) exhibited the same trend as OTU-indicated species richness.

**Table 3.** Correlations between *P. donghaiense* cell density and other environmental variables and diversity indices of dinoflagellate community, as measured with the rank correlation coefficient or Spearman's rho

	Number of OTUs	Shannon-Wiener index	Gini-Simpson index	Chao1 index
	Spearman rho ( <i>p</i> -level)			
<i>P. donghaiense</i> vs. diversity indices	-0.52 (<0.000 1***)	-0.67 (<0.000 1***)	-0.609 (0.001**)	-0.37 (0.001**)
Chl <i>a</i> vs. diversity indices	-0.43 (0.031*)	-0.51 (0.009*)	-0.56 (0.004*)	0.01 (0.007**)
Temperature vs. diversity indices	0.29 (0.156)	0.37 (0.069)	0.35 (0.088)	0.38 (0.059)
Salinity vs. diversity indices	0.16 (0.452)	0.23 (0.26)	0.22 (0.0286*)	0.37 (0.069)
Nitrite vs. diversity indices	0.62 (0.001**)	0.57 (0.003**)	0.53 (0.007**)	0.29 (0.15)
Nitrate vs. diversity indices	0.48 (0.015*)	0.48 (0.013*)	0.48 (0.014*)	0.07 (0.756)
TN vs. diversity indices	-0.62 (0.001**)	-0.72 (0.001**)	-0.76 (0.001**)	-0.43 (0.034*)
TP vs. diversity indices	-0.52 (0.007**)	-0.64 (0.001**)	-0.67 (<0.000 1***)	0.37 (0.73)
Phosphate vs. diversity indices	-0.009 (0.967)	0.01 (0.968)	-0.01 (0.971)	-0.29 (0.159)
Ammonium vs. diversity indices	0.24 (0.328)	0.03 (0.900)	-0.04 (0.85)	0.007 (0.97)

Note: The sample sizes for all were 50 ( $n=50$ ). \*  $0.01 < p < 0.05$ ; \*\*  $0.001 < p < 0.01$ ; \*\*\*  $p < 0.001$ .

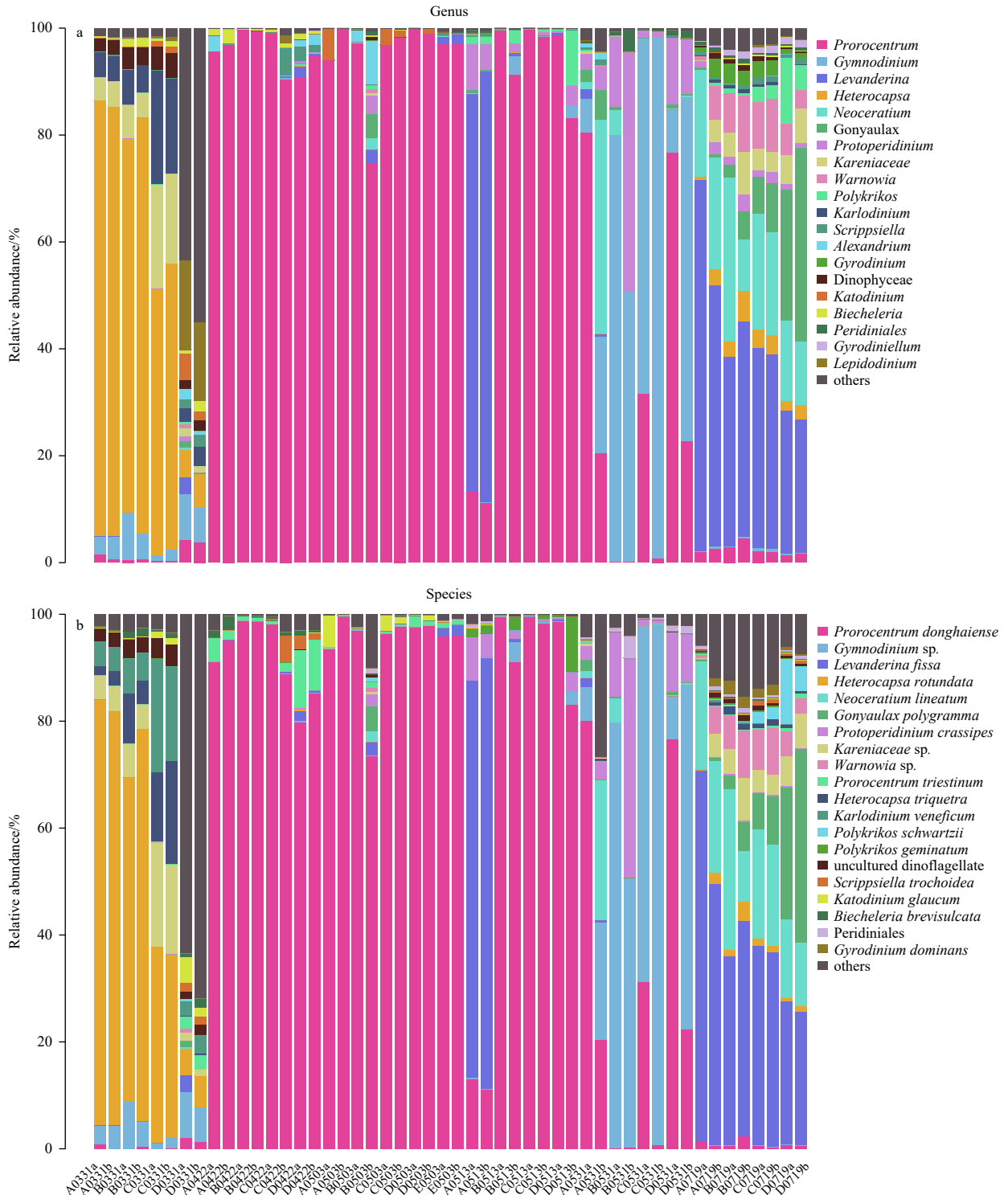


**Fig. 3.** Relative abundance of the top 20 genera (a) and species (b) of dinoflagellates in the 50 samples. The abundance is presented as percentage of each taxon in the total reads of valid sequences of all dinoflagellates in a sample. Note that “others” indicates the total of all other taxa except for the top 20 taxa (genera or species), which will allow a 100 percentage for all taxa. The annotations “uncultured dinoflagellate” was the original annotation of a reference sequence in the GenBank that was not convincingly identified to any particular genus or species.

**3.3 *Prorocentrum donghaiense* bloom negatively affected species diversity of the dinoflagellate community**

We determined if the species diversity of the dinoflagellate community was affected by the presence of *P. donghaiense*

bloom using the rank correlation coefficient or Spearman’s rho. Note that the alpha diversity indices here included species richness as expressed in the number of OTUs and Chao1 index, the Shannon index (indicating species evenness of community), and

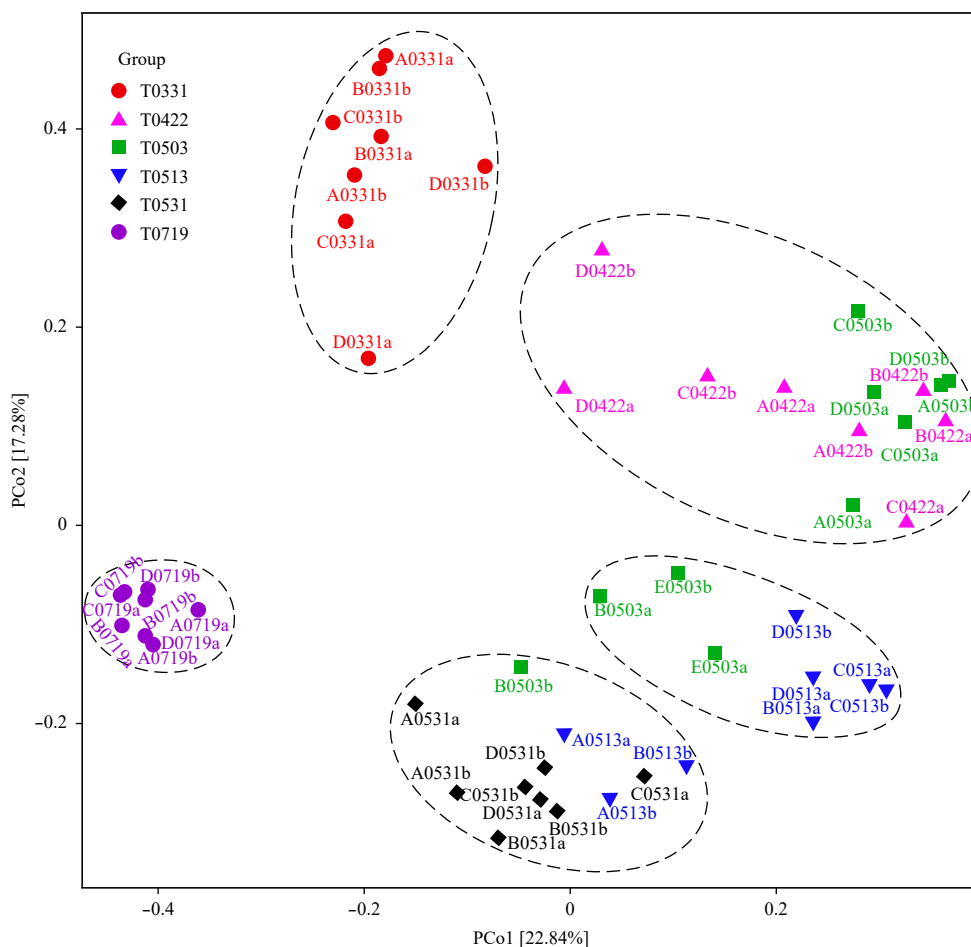


**Fig. 4.** Principal coordinates analysis (PCoA) plot on the Bray-Curtis distance matrix and depicting patterns of beta diversity for dinoflagellate communities of all samples. Different broken circles represent different clusters.

Gini-Simpson index ( $1-\lambda$ , indicating the probability that the two entities taken at random from a dataset of interest represent different species). It can be seen that all the number of OTUs, Chao1 index, Shannon-Wiener index, and Gini-Simpson index were negatively correlated with the cell density of *P. donghaiense* significantly (Table 3, Spearman's rho = -0.52, -0.67, -0.609, and -0.37, respectively;  $p < 0.001$ ). Because of the interactions of phytoplankton dynamics and ambient nutrients, the four indices were also significantly correlated with Chl *a*,  $\text{NO}_2^-$ -N,  $\text{NO}_3^-$ -N, TP, and TN, but not with  $\text{PO}_4^{3-}$ -P and  $\text{NH}_4^+$ -N (Table 3).

### 3.4 Dominant dinoflagellate groups varied among pre-, during and post-blooms of *P. donghaiense*

Metagenomic analysis revealed changes in the abundance of OTUs classifiable to various taxonomic levels, including shifts in dominant genera and species on date basis. The top 20 most abundant genera and species of each sample showed that 26 of the 50 samples were dominated by *Prorocentrum* (76.6%–99.6% of the top 20), while during the before-blooming period, the dinoflagellate community was dominated by *Heterocapsa\_rundata* (4.9%–79.6% dominance) that could not be well identified to any currently accepted genus of dinoflagellates (Fig. 3). All samples taken on April 22, May 3, and May 13 except for A0513a and A0513b were from blooming area and dominated by *P. donghaiense*. The samples of A0513a and A0513b were from non-blooming area and dominated by *Levanderina fissa*. After the

blooming period, all samples taken on July 19 were dominated by *L. fissa* for most of the samples (25.0%–69.3% dominance; Fig. 3).

### 3.5 Principal coordinates analysis (PCoA) and redundancy analysis (RDA)

Principal coordinates analysis was conducted to evaluate similarities among different surface samples at the OTU level. The PCoA results for all samples showed that all samples formed roughly five clusters: the samples of March 31, the samples of July 19, samples were each formed a tight cluster distinctly separated from other samples, while the samples of April 22 and May 03 (except for B0503a, B0503b, E0503a and E0503b) as one, the samples of May 13 (plus samples B0503a, E0503a and E0503b, except for A0513a, A0513b and B0513b) formed one cluster and the samples of May 31 (plus samples A0513a, A0513b, B0513b and B0503b) formed one cluster, respectively (Fig. 4), corresponding to the periods of before bloom (March 31), early bloom (April 22), bloom (May 3 and 13), and postal bloom (May 31 and July 19) of *P. donghaiense*. The samples that made the clusters expanded (i.e., part of the samples taken on April 22 and May 13) represented transitions of the blooming period. The location of samples B0503b and B0513b might be caused by experimental error or the duplicated samples differing greatly. The cluster of March 31 (plus samples D0422a and D0422b) represented transitions between before bloom and early bloom, while the cluster of May 31 (plus samples A0513a and A0513b) represented transitions



phytoplankton communities is the best predictor for resource use efficiency (e.g., nutrients) of phytoplankton and factors reducing phytoplankton diversity may have direct detrimental effects on the amount and predictability of aquatic primary production (Ptacnik et al., 2008). While environmental variables such as temperature, turbulence, and nutrient levels are generally the primary forces shaping the community structure and driving HABs (see the discussion below), a bloom can be a vital driving force by its own for the transition of phytoplankton community structure due to the biological features of the blooming species. For example, most of HABs-causing species have been demonstrated to be allelopathic to other co-occurring phytoplankton species via releasing allelochemicals (Felpeto et al., 2018; Leão et al., 2009; Leflaive and Ten-Hage, 2007). A blooming species generally can squeeze the living space of other species via fast growth, which will consequently reduce the nutrient and space availability to competitors.

#### 4.2 Effects of environmental variables on the dinoflagellate community

Our RDA results showed that *P. donghaiense* abundance,  $\text{NO}_3^-$ -N, and  $\text{SiO}_3^{2-}$  were the three most important environmental factors affecting the dinoflagellate community. *Prorocentrum donghaiense* abundance was correlated negatively to  $\text{NO}_3^-$ -N,  $\text{NO}_2^-$ -N,  $\text{PO}_4^{3-}$ -P,  $\text{NH}_4^+$ -N, temperature and salinity, but positively to TN, TP, Chl *a* and  $\text{SiO}_3^{2-}$ . Although dinoflagellates do not need  $\text{SiO}_3^{2-}$  for growth, the RDA results showed  $\text{SiO}_3^{2-}$  appeared to be one of those important factors in shaping the dinoflagellate community, which might be indirectly caused via the effects of  $\text{SiO}_3^{2-}$  on the transition of diatom community during the sampling period. The ratio of DIN to DIP tended to decrease along with the development and maintenance of bloom, and increase along with disappearance of bloom. At the beginning of the survey (March 31), the cell density of *P. donghaiense* was comparatively low (270 cells/mL), and the DIN to DIP ratio was 18–22, which was more suitable for the growth of *P. donghaiense* (Li et al., 2009), while, during the blooming period of *P. donghaiense*, the ratio showed a downward trend in general, possibly due to the different absorption rates for different nutrients by the bloom-forming organism (Zhang et al., 2008). This trend indicates a faster absorption rate of DIN by *P. donghaiense* and consequently a larger effect of DIN on the growth of *P. donghaiense*, compared to  $\text{PO}_4^{3-}$ -P. On May 13, the ratio reached the minimum, indicating a limiting level of DIN to the *P. donghaiense* growth (Li et al., 2014; Zhang et al., 2008). Supportively, it was observed there were significant negative correlations between TP and the four diversity indices (the number of OTUs, Shannon index, Gini-Simpson index, and Chao1 index), indicating that TP also stimulated the growth or bloom of *P. donghaiense*. However,  $\text{PO}_4^{3-}$  did not exhibit a significant correlation with these four diversity indices, indicating the utilization or uptake of P by *P. donghaiense* was not linearly correlated with the ambient concentration of  $\text{PO}_4^{3-}$ -P. Our RDA analysis revealed that, in addition to nutrients, temperature and salinity also made contributions to the transition of the dinoflagellate community, which is somehow in contrast to the recent result of Zhou et al. (2018) where temperature and salinity were two key environmental factors associated with changes in bacterial and archaeal community structure but not with variations in eukaryotic community. While it is well understandable that temperature acted as an important factor, the apparent correlation between salinity and *P. donghaiense* and the dinoflagellate community might be a good indication of nutrient input

from freshwater runoff.

In summary, our investigation observed that the bloom of *P. donghaiense* negatively affected bio-diversity in the dinoflagellate sub-community level both in reducing the species richness (as expressed in the number of OTUs and Chao1 index) and diversity indices (Shannon index and Gini-Simpson index). PCoA results showed that the dinoflagellate community during the blooming period of *P. donghaiense* differed significantly from the community before and after the blooming period. RDA analyses indicated that *P. donghaiense* abundance was the most important factor affecting the dinoflagellate community, which strongly indicates that the bloom of *P. donghaiense* played a vital role in shaping the dinoflagellate community structure, possibly via processes such as allelopathy (Ens et al., 2009; Leão et al., 2012), nutrient and space competition, and fast growth itself. Although these results are not beyond our anticipation, we believe the present work provides meaningful and solid evidence for the negative effects of HABs on the plankton community and coastal ecosystem based on a comprehensive series of field sampling and high throughput pyrosequencing.

#### References

- Anderson D M, Cembella A D, Hallegraeff G M. 2012. Progress in understanding harmful algal blooms: paradigm shifts and new technologies for research, monitoring, and management. *Annual Review of Marine Science*, 4: 143–176, doi: [10.1146/annurev-marine-120308-081121](https://doi.org/10.1146/annurev-marine-120308-081121)
- Anderson D M, Glibert P M, Burkholder J M. 2002. Harmful algal blooms and eutrophication: nutrient sources, composition, and consequences. *Estuaries*, 25: 704–726, doi: [10.1007/BF02804901](https://doi.org/10.1007/BF02804901)
- Aranda M, Li Y, Liew Y J, et al. 2016. Genomes of coral dinoflagellate symbionts highlight evolutionary adaptations conducive to a symbiotic lifestyle. *Scientific Reports*, 6: 39734, doi: [10.1038/srep39734](https://doi.org/10.1038/srep39734)
- Burkholder J M, Azanza R V, Sako Y. 2006. The ecology of harmful dinoflagellates. In: Granéli E, Turner J T, eds. *Ecology of Harmful Algae*. Berlin, Heidelberg: Springer, 53–66
- Chai Zhaoyang, He Zhili, Deng Yunyan, et al. 2018. Cultivation of seaweed *Gracilaria lemaneiformis* enhanced biodiversity in a eukaryotic plankton community as revealed via metagenomic analyses. *Molecular Ecology*, 27(4): 1081–1093, doi: [10.1111/mec.14496](https://doi.org/10.1111/mec.14496)
- Chai Zhaoyang, Wang Huan, Deng Yunyan, et al. 2020. Harmful algal blooms significantly reduce the resource use efficiency in a coastal plankton community. *Science of The Total Environment*, 704: 135381, doi: [10.1016/j.scitotenv.2019.135381](https://doi.org/10.1016/j.scitotenv.2019.135381)
- Cui Lei, Lu Xinxin, Dong Yuele, et al. 2018. Relationship between phytoplankton community succession and environmental parameters in Qinhuangdao coastal areas, China: a region with recurrent brown tide outbreaks. *Ecotoxicology and Environmental Safety*, 159: 85–93, doi: [10.1016/j.ecoenv.2018.04.043](https://doi.org/10.1016/j.ecoenv.2018.04.043)
- Ens E J, French K, Bremner J B. 2009. Evidence for allelopathy as a mechanism of community composition change by an invasive exotic shrub, *Chrysanthemoides monilifera* spp. *rotundata*. *Plant and Soil*, 316(1–2): 125–137, doi: [10.1007/s11104-008-9765-3](https://doi.org/10.1007/s11104-008-9765-3)
- Felpeto A B, Roy S, Vasconcelos V M. 2018. Allelopathy prevents competitive exclusion and promotes phytoplankton biodiversity. *Oikos*, 127(1): 85–98, doi: [10.1111/oik.04046](https://doi.org/10.1111/oik.04046)
- Huse S M, Dethlefsen L, Huber J A, et al. 2008. Exploring microbial diversity and taxonomy using SSU rRNA hypervariable tag sequencing. *PLoS Genetics*, 4(11): e1000255, doi: [10.1371/journal.pgen.1000255](https://doi.org/10.1371/journal.pgen.1000255)
- JOGFS International Project Office. 1994. JOGFS report No. 19. protocols for the Joint Global Ocean Flux Studies (JGOFS) core measurements. Bergen, Norway: JOGFS International Project Office, Center for Studies of Environment and Resources
- Jonsson P R, Pavia H, Toth G. 2009. Formation of harmful algal

- blooms cannot be explained by allelopathic interactions. Proceedings of the National Academy of Sciences of the United States of America, 106(27): 11177–11182, doi: [10.1073/pnas.0900964106](https://doi.org/10.1073/pnas.0900964106)
- Landsberg J H. 2002. The effects of harmful algal blooms on aquatic organisms. *Reviews in Fisheries Science*, 10(2): 113–390, doi: [10.1080/20026491051695](https://doi.org/10.1080/20026491051695)
- Leão P N, Ramos V, Vale M, et al. 2012. Microbial community changes elicited by exposure to cyanobacterial allelochemicals. *Microbial Ecology*, 63(1): 85–95, doi: [10.1007/s00248-011-9939-z](https://doi.org/10.1007/s00248-011-9939-z)
- Leão P N, Vasconcelos M T S D, Vasconcelos V M. 2009. Allelopathy in freshwater cyanobacteria. *Critical Reviews in Microbiology*, 35(4): 271–282, doi: [10.3109/10408410902823705](https://doi.org/10.3109/10408410902823705)
- Leflaive J, Ten-Hage L. 2007. Algal and cyanobacterial secondary metabolites in freshwaters: a comparison of allelopathic compounds and toxins. *Freshwater Biology*, 52(2): 199–214, doi: [10.1111/j.1365-2427.2006.01689.x](https://doi.org/10.1111/j.1365-2427.2006.01689.x)
- Legendre P, Oksanen J, ter Braak C J F. 2011. Testing the significance of canonical axes in redundancy analysis. *Methods in Ecology and Evolution*, 2(3): 269–277, doi: [10.1111/j.2041-210X.2010.00078.x](https://doi.org/10.1111/j.2041-210X.2010.00078.x)
- Li Hongmei, Tang Hongjie, Shi Xiaoyong, et al. 2014. Increased nutrient loads from the Changjiang (Yangtze) River have led to increased Harmful Algal Blooms. *Harmful Algae*, 39: 92–101, doi: [10.1016/j.hal.2014.07.002](https://doi.org/10.1016/j.hal.2014.07.002)
- Li Ji, Glibert P M, Zhou Mingjiang, et al. 2009. Relationships between nitrogen and phosphorus forms and ratios and the development of dinoflagellate blooms in the East China Sea. *Marine Ecology Progress Series*, 383: 11–26, doi: [10.3354/meps07975](https://doi.org/10.3354/meps07975)
- Lin Senjie, Cheng Shifeng, Song Bo, et al. 2015. The *Symbiodinium kawagutii* genome illuminates dinoflagellate gene expression and coral symbiosis. *Science*, 350(6261): 691–694, doi: [10.1126/science.aad0408](https://doi.org/10.1126/science.aad0408)
- Lin Jianing, Yan Tian, Zhang Qingchun, et al. 2014. *In situ* detrimental impacts of *Prorocentrum donghaiense* blooms on zooplankton in the East China Sea. *Marine Pollution Bulletin*, 88(1–2): 302–310, doi: [10.1016/j.marpolbul.2014.08.026](https://doi.org/10.1016/j.marpolbul.2014.08.026)
- Lu Douding, Goebel J, Qi Yuzao, et al. 2005. Morphological and genetic study of *Prorocentrum donghaiense* Lu from the East China Sea, and comparison with some related *Prorocentrum* species. *Harmful Algae*, 4(3): 493–505, doi: [10.1016/j.hal.2004.08.015](https://doi.org/10.1016/j.hal.2004.08.015)
- Miao Yu, Wang Zhu, Liao Runhua, et al. 2017. Assessment of phenol effect on microbial community structure and function in an anaerobic denitrifying process treating high concentration nitrate wastewater. *Chemical Engineering Journal*, 330: 757–763, doi: [10.1016/j.cej.2017.08.011](https://doi.org/10.1016/j.cej.2017.08.011)
- Parsons T R, Maita Y, Lalli C M. 1984. *A Manual of Chemical & Biological Methods for Seawater Analysis*. Oxford: Pergamon Press, 423–453
- Ptacnik R, Solimini A G, Andersen T, et al. 2008. Diversity predicts stability and resource use efficiency in natural phytoplankton communities. *Proceedings of the National Academy of Sciences of the United States of America*, 105(13): 5134–5138, doi: [10.1073/pnas.0708328105](https://doi.org/10.1073/pnas.0708328105)
- Rozen S, Skaletsky H. 2000. Primer3 on the WWW for general users and for biologist programmers. In: Misener S, Krawetz S A, eds. *Bioinformatics Methods and Protocols*. Totowa: Humana Press, 365–386
- Schneider A R, Gommeaux M, Duclercq J, et al. 2017. Response of bacterial communities to Pb smelter pollution in contrasting soils. *Science of the Total Environment*, 605–606: 436–444, doi: [10.1016/j.scitotenv.2017.06.159](https://doi.org/10.1016/j.scitotenv.2017.06.159)
- Smayda T J. 1990. Novel and nuisance phytoplankton blooms in the sea: evidence for a global epidemic. In: Granéli E, Sundström B, Edler L, et al., eds. *Toxic Marine Phytoplankton*. New York, USA: Elsevier, 29–40
- Smayda T J. 1997. Harmful algal blooms: their ecophysiology and general relevance to phytoplankton blooms in the sea. *Limnology and Oceanography*, 42: 1137–1153, doi: [10.4319/lo.1997.42.5\\_part\\_2.1137](https://doi.org/10.4319/lo.1997.42.5_part_2.1137)
- State Oceanic Administration. 2001–2015. Bulletin of marine disaster of China (in Chinese). <http://www.mnr.gov.cn/sj/sjfw/hy/gbgs/zghyzhgb> [2019-12-03/2020-02-24]
- Sun Zhen, Li Guoping, Wang Chengwei, et al. 2014. Community dynamics of prokaryotic and eukaryotic microbes in an estuary reservoir. *Scientific Reports*, 4: 6966
- Sunagawa S, Coelho L P, Chaffron S, et al. 2015. Structure and function of the global ocean microbiome. *Science*, 348(6237): 1261359, doi: [10.1126/science.1261359](https://doi.org/10.1126/science.1261359)
- Valderrama J C. 1981. The simultaneous analysis of total nitrogen and total phosphorus in natural waters. *Marine Chemistry*, 10(2): 109–122, doi: [10.1016/0304-4203\(81\)90027-X](https://doi.org/10.1016/0304-4203(81)90027-X)
- Vaulot D, Eikrem W, Viprey M, et al. 2008. The diversity of small eukaryotic phytoplankton ( $\leq 3 \mu\text{m}$ ) in marine ecosystems. *FEMS Microbiology Reviews*, 32(5): 795–820, doi: [10.1111/j.1574-6976.2008.00121.x](https://doi.org/10.1111/j.1574-6976.2008.00121.x)
- West T L, Marshall H G, Tester P A. 1996. Natural phytoplankton community responses to a bloom of the toxic dinoflagellate *Gymnodinium breve Davis* off the North Carolina coast. *Castanea*, 61(4): 356–368
- Xu Ning, Duan Shunshan, Li Aifen, et al. 2010. Effects of temperature, salinity and irradiance on the growth of the harmful dinoflagellate *Prorocentrum donghaiense* Lu. *Harmful Algae*, 9(1): 13–17, doi: [10.1016/j.hal.2009.06.002](https://doi.org/10.1016/j.hal.2009.06.002)
- Xu Xin, Yu Zhiming, Cheng Fangjin, et al. 2017. Molecular diversity and ecological characteristics of the eukaryotic phytoplankton community in the coastal waters of the Bohai Sea, China. *Harmful Algae*, 61: 13–22, doi: [10.1016/j.hal.2016.11.005](https://doi.org/10.1016/j.hal.2016.11.005)
- Yao Weiming, Li Chao, Gao Junzhang. 2006. Red tide plankton along the south coastal area in Zhejiang province. *Marine Science Bulletin (in Chinese)*, 25(3): 87–91
- Zhang Chuansong, Wang Jiangtao, Zhu Dedi, et al. 2008. The preliminary analysis of nutrients in harmful algal blooms in the East China Sea in the spring and summer of 2005. *Haiyang Xuebao (in Chinese)*, 30(3): 153–159
- Zhou Jin, Richlen M L, Sehein T R, et al. 2018. Microbial community structure and associations during a marine dinoflagellate bloom. *Frontiers in Microbiology*, 9: 1201, doi: [10.3389/fmicb.2018.01201](https://doi.org/10.3389/fmicb.2018.01201)

## Supplementary information:

**Table S1.** Biological and abiotic variables in different phases of the bloom series (mean $\pm$ SD).

**Table S2.** Number of reads and OTUs during the analysis process in the dinoflagellate community.

The supplementary information is available online at <https://doi.org/10.1007/s13131-020-1585-1>. The supplementary information is published as submitted, without typesetting or editing. The responsibility for scientific accuracy and content remains entirely with the authors.